Desalination and Water Treatment
www.deswater.com

1944-3994/1944-3986 © 2012 Desalination Publications. All rights reserved
doi: 10.1080/19443994.2012.698809

Taylor & Francis
Taylor & Francis Group

48 (2012) 163–173
October

Studies on the removal of arsenate from water through electrocoagulation using direct and alternating current

Subramanyan Vasudevan*, Jothinathan Lakshmi, Ganapathy Sozhan

CSIR – Central Electrochemical Research Institute (CSIR), Karaikudi 630 006, India
Tel. +91 4565 227556; Fax: +91 4565 227779; email: vasudevan65@gmail.com

Received 3 September 2011; Accepted 24 April 2012

ABSTRACT

Using alternating current in an electrocoagulation process offers an alternative to conventional electrocoagulation processes, where the direct current is used. The main objective of the present investigation is to study the effects of alternating current (AC) and direct current (DC) on the removal efficiency of arsenate by electrocoagulation using magnesium as anode and cathode. The effect of current density, solution pH, temperature, co-existing ions, adsorption isotherm and kinetics has been studied. The optimum removal efficiency of 98.3% and 97.9% was achieved with the energy consumption of 0.724 and 1.035 kWh/m^3 at a current density of 0.2 A/dm^2, at pH of 7.0 for AC and DC, respectively. The adsorption of arsenate preferably fitting the Langmuir adsorption isotherm suggests monolayer coverage of adsorbed molecules for both AC and DC. The adsorption process follows second-order kinetics model with good correlation coefficient. Temperature studies showed that adsorption was endothermic and spontaneous in nature.

Keywords: Electrocoagulation; Alternating/direct current; Arsenate; Adsorption; Kinetics; Thermodynamics

1. Introduction

Arsenic, which is toxic to man and other living organisms, presents potentially serious environmental problems throughout the world. Unfortunately, there is no known cure for arsenic poisoning and therefore providing arsenic-free drinking water is the only way to diminish the adverse health effects of arsenic. Arsenic is an environmental health concern, because long-term epidemiological studies demonstrate that it is toxic to humans and other living organisms. Arsenic from natural and anthropic sources has gotten into many water sources, especially groundwater sources. These anthropic sources of arsenic are metallurgical industries, glassware and ceramic production, tannery operation, dyestuff, pesticide industries, some organic and inorganic chemical manufacturing, petroleum refining and rare earth metals. As a result both the inorganic and organic arsenic compounds can be found in soil, plants, animals and humans [1].

Arsenic in natural waters is a worldwide problem. Arsenic pollution has been reported recently in USA, China, Chile, Bangladesh, Taiwan, Mexico, Argentina, Poland, Canada, Hungary, New Zealand, Japan and India [2]. Inorganic arsenic is predominantly present in natural waters. Arsenate [As(V)] and arsenite [As(III)] are primary forms of arsenic in soils and natural waters. As(III) is more mobile in groundwater and 25–60 times

*Corresponding author.

more toxic than As(V) [2]. The concentration of arsenic species is mainly dependent on redox potentials and pH. Under low pH and mildly reducing conditions, As(III) is thermodynamically stable and exists as arsenious acid (H_3AsO_3, $H_2AsO_3^-$, $HAsO_3^{2-}$, AsO_3^{3-}) [3]. Under oxidizing conditions, the predominant species is As(V) which exists as arsenic acid (H_3AsO_4, $H_2AsO_4^-$, $HAsO_4^{2-}$, AsO_4^3) as stable species in the pH interval 3–6, 7–11, and 12–14, respectively [4,5]. Pollution-based studies have shown that arsenate may adversely affect several organs in the human body including cancer of the skin, lung and urinary bladder. United States Environmental Production Agency (USEPA) lowered the maximum concentration level of arsenic in water system to 20 ppb [6]. Consequently, the removal of arsenic from water system becomes urgent in order to comply with the legislation [7].

Conventional methods for removing heavy metal ions from aqueous solution include chemical precipitation, chemical oxidation or reduction, filtration, ion exchange, application of membrane technology, and electro dialysis (ED) [8–14]. However, these processes have considerable disadvantages including incomplete metal removal, requirements for expensive equipment and monitoring system, high reagent and energy requirements or generation of toxic sludge or other waste products that require disposal. During the last few decades electrochemical water treatment technologies have undergone rapid growth and development. One of these technologies is the electrochemically assisted coagulation that can compete with the conventional chemical coagulation process. Electrocoagulation is an emerging water treatment technology that has been applied successfully to treat various wastewaters [15]. It has been applied for treatment of potable water. Further, electrocoagulation offers possibility of anodic oxidation and in situ generation of adsorbents. The electrochemical production of destabilization agents that brings charge neutralization from pollutant and it has been used for water or wastewater treatment. It has been successfully used to treat oil wastes, with high removal efficiencies as high as 99% [16]. Usually iron and aluminum plates are used as electrodes in the electrocoagulation followed by electrosorption process. The advantages of electrocoagulation include high particulate removal efficiency, a compact treatment facility, relatively low cost, and the possibility of complete automation [20–25]. This technique does not require supplementary addition of chemicals and reduces the volume of produced sludge. The electrochemical reactions with metal M as anode may be summarized as follows,

At anode:

$$M_{(s)} \rightarrow M_{(aq)}^{n+} + ne^- \quad (1)$$

$$2H_2O_{(l)} \rightarrow 4H_{(aq)}^{+} + O_{2(g)}^{+} + 4e^- \quad (1a)$$

At cathode:

$$M_{(aq)}^{n+} + ne^- \rightarrow M_{(s)} \quad (2)$$

$$2H_2O_{(l)} + 2e^- \rightarrow H_{2(g)} + 2OH^- \quad (2a)$$

If Fe or Al electrodes are used, the generated $Fe_{(aq)}^{3+}$ or $Al_{(aq)}^{3+}$ ions will immediately undergo further spontaneous reactions to produce corresponding hydroxides and/or polyhydroxides. These hydroxides/polyhydroxides/polyhydroxy metallic compounds have a strong affinity with dispersed/dissolved ions as well as the counter ions to cause coagulation/adsorption. This method is characterized by reduced sludge production, a minimum requirement of chemicals, and ease of operation [17–19].

Usually direct current (DC) is used in an electrocoagulation processes. In this case, an impermeable oxide layer may form on the cathode as well as corrosion formation on the anode due to oxidation. These prevent the effective current transport between the anode and cathode, so the efficiency of electrocoagulation processes declines. These disadvantages of using DC have been overcome by adopting alternating current (AC) in electrocoagulation processes. The main objective of this study is to investigate the effect of AC on the removal efficiency of arsenate using magnesium as anode and cathode. The effect of the initial concentration of arsenate ion, pH, temperature, current density and coexisting ions were investigated. The adsorption kinetics of arsenate ions on magnesium hydroxide is also studied. For this, equilibrium adsorption behavior is analyzed by fitting the Langmuir and Freundlich isotherm models. The adsorption kinetics of electrocoagulation was analyzed using first- and second-order kinetic models. Finally, the effects of temperature were studied to determine the nature of adsorption. Although, there are numerous reports related with electrochemical coagulation as a means of removal of many pollutants from water and wastewater, but there are limited work on arsenic removal by electrochemical method and its adsorption and kinetics studies.

2. Experimental

2.1. Cell construction and electrolysis

The electrolytic cell consists of a 1.0-L Plexiglas vessel that was fitted with a polycarbonate cell cover with slots to introduce the anode, cathode, pH sensor, a thermometer and electrolytes. Magnesium with surface area

0.2 dm^2 acted as the anode and cathode of same size were placed at an inter-electrode distance of 0.005 m. Thermodynamic studies were carried out at 313–343 K. The temperature of the electrolyte has been controlled to the desired value with a variation of ±2 K by adjusting the rate of flow of thermostatically controlled water through an external glass-cooling spiral. A regulated direct current (DC) was supplied from a rectifier (10 A, 0–25 V; Aplab model) and regulated alternating current (AC) was supplied from a source (0–5 A, 0–270 V, 50 Hz; AMETEK Model: EC1000S).

Sodium arsenate ($Na_2HAsO_4{\cdot}7H_2O$) (Analar Reagent, Merck, Germany) was dissolved in deionized water for the required concentration (0.5–1.5 mg/L). The solution of 0.90 L was used for each experiment as the electrolyte. The pH of the electrolyte was adjusted, if required, with HCl or NaOH solutions (AR Grade, Merck, Germany) before electrolysis starts. To study the effect of co-existing ions in the removal of As(V), sodium salts (Analar Grade) of phosphate (0–50 mg/L), silicate (0–15 mg/L), carbonate (0–250 mg/L) and fluoride (0–5 mg/L) were added to the electrolyte.

2.2. Analytical method

Ion Chromatography (Metrohm AG, Switzerland) was used to determine the concentration of arsenate. The SEM and EDAX of magnesium hydroxide were analyzed with a Scanning Electron Microscope (SEM) made by **Hitachi (model s-3000h)**. The XRD of electrocoagulatioan-by products were analyzed by a JEOL X-ray diffractometer (Type – JEOL, Japan). The Fourier transform infrared spectrum of magnesium hydroxide was obtained using **Nexus 670 FTIR** spectrometer (**Thermo Electron Corporation, USA)**. The concentration of carbonate, fluoride, silicate and phosphate were determined using UV–Visible Spectrophotometer (MERCK, Pharo 300, Germany).

3. Result and discussion

3.1. Effect of current density

Among the various operating variables, current density is an important factor which strongly influences the performance of electrocoagulation. The effect of current density on the removal efficiency of As(V) ions was studied at 0.05, 0.1, 0.2, 0.3, 0.4 A/dm^2 at an initial concentration of 0.5 mg/L of arsenate at pH 7.0 using both AC and DC source. The results showed that the optimum removal efficiency of 98.3% and 97.9% with the energy consumption of 0.724 and 1.035 kWh/m^3 was achieved at a current density of 0.2 A/dm^2, at pH of 7.0 using AC and DC, respectively. Table 1 show that the removal efficiency of As(V) was higher and energy consumption was lower in the case of AC than DC. This may be due to the uniform dissolution of anode during electrocoagulation in the case of AC. This is due to sufficient current through the solution; the metal ions generated by the dissolution of the sacrificial electrode were hydrolyzed to form a series of metallic hydroxide species. The amount of solubilized magnesium hydroxide increases linearly with the current density according to the Faraday law [26]. As expected, the amount of arsenate adsorption increases with the increase in adsorbent concentration, which indicates that the adsorption depends upon the availability of binding sites for arsenate.

3.2. Effect of pH

It has been established that the influent pH is an important operating factor influencing the performance of electrochemical processes. In order to examine the effect of the initial pH for AC and DC source, experiments were carried out in acidic (pH 2.0), slightly acidic (pH 5), neutral (pH 7.0), and alkaline (pH 10.0) media having 0.5 mg/L of arsenate containing solutions. The percentage of arsenate adsorption was maximum at

Table 1
Effect of current density on the removal efficiency of arsenate from drinking water at temperature 305 K and pH 7

Current density (A/dm^2)	AC		DC	
	Removal efficiency (%)	Energy consumption (kWh/kL)	Removal efficiency (%)	Energy consumption (kWh/kL)
0.05	92	0.441	90	0.667
0.1	94.5	0.623	92.6	0.864
0.2	98.3	0.724	97.9	1.035
0.3	98.6	0.995	98	1.246
0.4	98.8	1.122	98.2	1.331

pH 7, a decreasing trend in adsorption was observed when below and above pH 7 for both AC and DC source. At an initial concentration of 0.5 mg/L, maximum adsorption of 98.3% and 97.9% at pH 7 for AC and DC source, respectively, was observed (Fig. 1). It can be seen from Fig. 1 that arsenate removal efficiencies increased with increasing pH and highest removal efficiencies were obtained at pH 7.0. The high efficiency of arsenate removal at neutral pH might be ascribed to the precipitation of their hydroxides at the cathode.

3.3. Effect of initial arsenate concentration

In order to evaluate the effect of initial arsenate concentration, experiments were conducted at varying initial concentration from 0.5 to 1.5 mg/L using AC and DC. Fig. 2 shows that the uptake of arsenate (mg/g) increased with increase in arsenate concentration per gram of $Mg(OH)_2$ and remained nearly constant after equilibrium time. The equilibrium time was found to be 10 min for all concentration studied. The amount of arsenate adsorbed (q_e) increased from 0.403 to 1.326 mgAs/g as the concentration increased from 0.5 to 1.5 mg/L for the AC source. The amount of adsorbed q_e increases with the increasing concentration of arsenate and reaches a saturation point when the active sites are fully covered with the adsorbate species [27]. The plots are single, smooth and continuous curves leading to saturation, suggesting the possible monolayer coverage to arsenate on the surface of the adsorbent. In the case of DC the equilibrium time was found to be 25 min for all concentration studied (figure not shown).

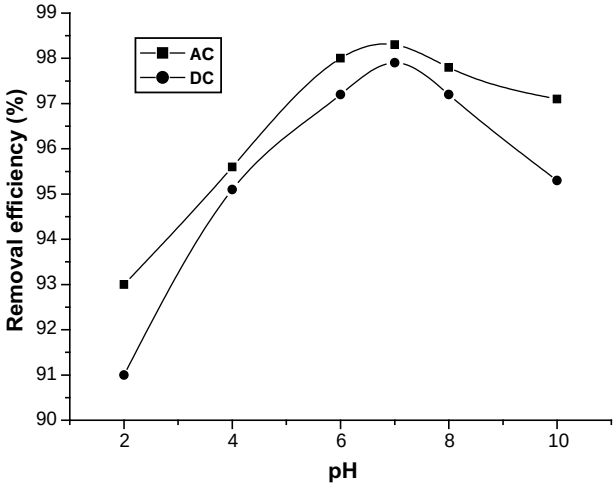

Fig. 1. Effect of pH on the removal efficiency of arsenate for AC and DC. Concentration of arsenate is 0.5 mg/L and electrolyte temperature is 303 K.

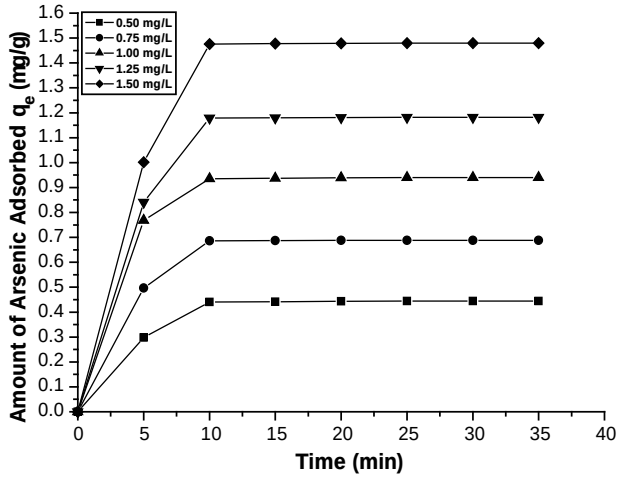

Fig. 2. Effect of electrolysis time and amount of arsenate adsorbed. Current density is 0.2 A/dm^2, pH is 7.0 and electrolyte temperature is 303 K.

3.4. Adsorption kinetics

In order to establish kinetic of arsenate adsorption, adsorption kinetics of magnesium anode was investigated by using first-order and second-order kinetic models with AC and DC.

3.4.1. First-order Lagergren model

The first order Lagergren model is generally expressed as follows [28,29]:

$$dq_t / dt = k_1(q_e - q_t) \quad (3)$$

where, q_t is the amount of arsenate adsorbed on the adsorbent at time t (min) and k_1 (min^{-1}) is the rate constant of first-order adsorption. The integrated form of the above equation with the boundary conditions $t = 0$ to $t > 0$ ($q = 0$ to $q > 0$) and then rearranged to obtain the following time dependence function:

$$\log(q_e - q_t) = \log(q_e) - k_1 t / 2.303 \quad (4)$$

where q_e is the amount of arsenate adsorbed at equilibrium. The values of $\log(q_e - q_t)$ were linearly correlated with t. The plot of log $(q_e - q_t)$ vs t (figure not shown) should give the linear relationship from which k_1 and q_e can be determined by the slope and intercept, respectively. Table 2 shows the computed results of first-order kinetics. A large difference of q_e between the experimental and calculated values and low correlation coefficient values indicates a poor first-order fit for the adsorption kinetics.

Table 2
Comparison between the experimental and calculated q_e values for different initialarsenate concentrations in first order adsorption kinetics at temperature 305 K and pH 7

Current source	Concentration (mg/L)	q_e (exp)	First-order adsorption			Second-order adsorption		
			q_e (cal)	$K_1 \times 10^3$ (min/mg)	R^2	q_e (cal)	$K_2 \times 10^3$ (min/mg)	R^2
AC	0.5	0.441	0.662	0.147	0.7942	0.437	0.1357	0.9998
	0.75	0.686	0.799	0.139	0.7465	0.679	0.1942	0.9989
	1.0	0.935	0.843	0.094	0.7689	0.931	0.2468	0.9993
	1.25	1.179	0.934	0.066	0.7566	1.165	0.3657	0.9956
	1.5	1.476	0.986	0.057	0.7984	1.460	0.5465	0.9996
DC	0.5	0.436	0.642	0.133	0.7651	0.430	0.1243	0.9999
	0.75	0.679	0.781	0.127	0.7825	0.666	0.1441	0.9845
	1.0	0.928	0.839	0.101	0.7733	0.926	0.1987	0.9925
	1.25	1.171	0.926	0.083	0.7891	1.166	0.2493	0.9999
	1.5	1.464	0.971	0.064	0.8021	1.472	0.2866	0.9998

3.4.2. Second-order Lagergren model

The second-order kinetic model is expressed as [30–33]

$$dq_t / dt = k_2(q_e - q_t)^2 \quad (5)$$

where k_2 is the rate constant of second order adsorption. The integrated form of Eq. (5) with the boundary condition $t = 0$ to >0 ($q = 0$ to >0) is

$$1/(q_e - q_t) = 1/q_e + k_2 t \quad (6)$$

Eq. (6) can be rearranged and linearized as

$$t/q_t = 1/k_2 q_e^2 + t/q_e \quad (7)$$

The plot of t/q_t and time (t) (Fig. 3) gave a linear relationship from which q_e and k_2 can be determined from the slope and intercept of the plot with high regression co-efficient (Table 2).

Table 2 depicts the computed results obtained from first- and second-order kinetic models for AC and DC source. The calculated q_e values well agree with the experimental q_e values for second-order kinetics model better than the first-order kinetics model for both AC and DC. These results indicate that the adsorption system belongs to the second-order kinetic model with high correlation coefficient values.

3.5. Adsorption isotherm

The adsorption capacity of the magnesium hydroxide has been tested using Freundlich, Langmuir and Dubinin–Radushkevich isotherms. To determine the isotherms, the initial pH was kept at 7 and the concentration of arsenate used was in the range of 0.5–1.5 mg/L using AC and DC sources.

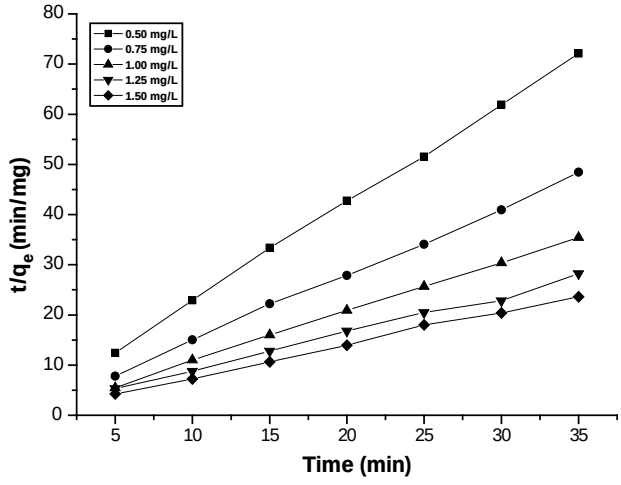

Fig. 3. Second-order kinetic model plot of different concentrations of arsenate. Current density is 0.2 A/dm², electrolyte temperature is 303 K and pH is 7.0.

3.5.1. Freundlich isotherm

The general form of Freundlich adsorption isotherm is represented by [34]

$$q_e = KC_e^n \quad (8)$$

Eq. (8) can be linearized in logarithmic form and the Freundlich constants can be determined as follows:

$$\log q_e = \log k_f + n \log C_e^n \quad (9)$$

where k_f is the Freundlich constant related to adsorption capacity, 'n' is the energy or intensity of adsorption and 'C_e' is the equilibrium concentration of arsenate (mg/L). The values of k_f and 'n' can be obtained by plotting logarithms of adsorption capacity against equilibrium concentrations. To determine the isotherms, the arsenate concentration used was 0.5–1.5 mg/L and at an initial pH 7. From the analysis of the results it is found that the Freundlich plots fit satisfactorily with the experimental data obtained in the present study (Table 3). This is well agreed with the results presented in the literature for adsorption of arsenate [8,35].

3.5.2. Langmuir isotherm

The linearized form of Langmuir adsorption isotherm model is [36].

$$C_e / q_e = 1 / q_0 b + C_e / q_e \quad (10)$$

where 'C_e' is the concentration of the arsenate solution (mg/L) at equilibrium, q_e the amount of arsenate adsorbed at equilibrium (mg/g), q_0 is the adsorption capacity (Langmuir constant) and 'b' is the energy of adsorption. Fig. 4 shows the Langmuir plot with experimental data. The value of the adsorption capacity 'q_m' as found to be 28.654 mg/g and 25.387 mg/g for AC and DC.

The essential characteristics of the Langmuir isotherm can be expressed as the dimensionless constant R_L

$$R_L = 1 / (1 + bC_0) \quad (11)$$

where R_L is the equilibrium constant indicating the type of adsorption, b and C_0 are the Langmuir constant and initial arsenate concentration, respectively. The R_L values between 0 and 1 indicate the favorable adsorption. The R_L values were found to be between 0 and 1 for all the concentration of arsenate studied. The results are presented in Table 3.

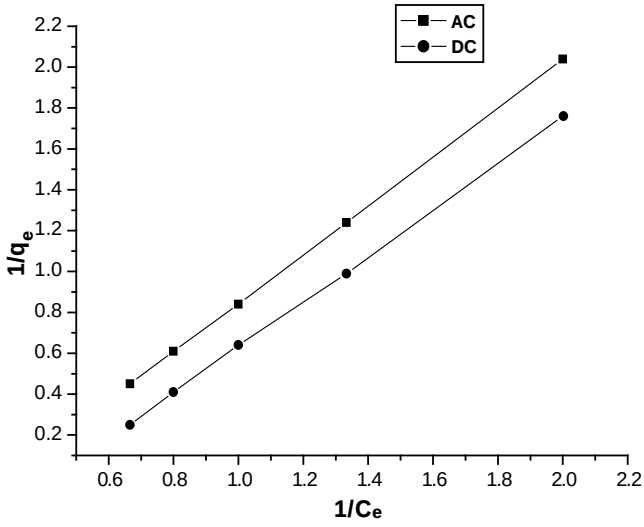

Fig. 4. Langmuir plot for adsorption of arsenate. pH is 7.0, Current density is 0.2 A/dm², electrolyte temperature is 303 K and concentration is 0.5–1.5 mg/L for AC and DC.

Table 3
Constant parameters and correlation coefficient calculated for different adsorption isotherm models for arsenate adsorption at 0.5 mg/L at 305 K

Isotherm		Constants			
		q_m (mg/g)	b (L/mg)	R_L	R^2
Langmuir	AC	28.654	0.0791	0.8561	0.9991
	DC	25.387	0.0766	0.8555	0.9995
		K_f (mg/g)	n (L/mg)	R^2	
Freundlich	AC	1.431	1.109	0.9881	
	DC	1.366	1.044	0.9896	
		Q_s (x10³ mol/g)	B (x10³ mol²/kJ²)	E (kJ/mol)	R^2
D–R	AC	0.761	0.2882	18.28	0.8336
	DC	0.661	0.2167	15.13	0.8456

3.5.3. Dubinin–Radushkevich (D–R) isotherm

This model is represented by [38]

$$q_e = q_s \exp(-B\varepsilon^2) \quad (12)$$

where $\varepsilon = RT \ln [1+1/C_e]$, B is related to the free energy of sorption per mole of the adsorbate as it migrates to the surface of the electrocoagulant ($Mg(OH)_2$) from infinite distance in the solution and q_s is the Dubinin–Radushkevich (D–R) isotherm constant related to the degree of adsorbate adsorption by the adsorbent surface. The linearized form of Eq. (12)

$$\ln q_e = \ln q_s - 2B \cdot RT \cdot \ln[1+1/C_e] \quad (13)$$

The isotherm constants of q_s and 'B' are obtained from the intercept and slope of the plot of $\ln q_e$ versus ε^2, respectively [39]. The constant 'B' gives the mean free energy 'E', of adsorption per molecule of the adsorbate when it is transferred to the surface of the solid

$$E = [1/\sqrt{2B}] \quad (14)$$

The magnitude of E is useful for estimating the type of adsorption process. It was found to be 18.28 kJ/mol and 15.13 kJ/mol for AC and DC source, which is bigger than the energy range of adsorption reaction, 8–16 kJ/mol [40]. So the type of adsorption of arsenate on magnesium was defined as chemical adsorption.

The correlation coefficient values of different isotherm models are listed in Table 3. The Langmuir isotherm model has higher regression co-efficient (R^2 = 0.999) when compared to the other models for both AC and DC. The adsorption data show good fit to the Langmuir than Freundlich as depicted by the regression coefficient for these systems for both AC and DC. R_L values between 0 and 1.0 further indicate a favorable adsorption of arsenate.

3.6. Effect of temperature

The amount of arsenate adsorbed on the adsorbent ($Mg(OH)_2$) increases by increasing the temperature indicating the process to be endothermic. The diffusion coefficient (D) for intraparticle transport of arsenate species into the adsorbent particles has been calculated at different temperature by

$$t_{1/2} = 0.03Xr_0^2 / D \quad (15)$$

where $t_{1/2}$ is the time of half adsorption (s), r_0 is the radius of the adsorbent particle (cm), D is the diffusion co-efficient in cm^2/s. For all chemisorption system the diffusivity co-efficient should be 10^{-5} to 10^{-13} cm^2/s [41,42]. In the present work, D is found to be in the range of 10^{-10} cm^2/s. The pore diffusion coefficient (D) values for various temperatures and different initial concentrations of arsenate are presented in Table 4.

To find out the energy of activation for adsorption of arsenate, the second-order rate constant is expressed in Arhenius form [43]

$$\ln k_2 = \ln k_0 - E/RT \quad (16)$$

where k_0 is the constant of the equation (g/mg/min), E is the energy of activation (J/mol), R is the gas constant (8.314 J/mol/K) and T is the temperature in K. Table 5 shows that the rate constants vary with temperature according to Eq. (16). The activation energy (16.45 kJ/mol and 12.36 kJ/mol for AC and DC) is calculated from slope of log k_2 vs $1/T$ (figure not shown). The free energy change is obtained using the following relationship:

$$\Delta G = -RT \ln K_c \quad (17)$$

where ΔG is the free energy (kJ/mol), K_c is the equilibrium constant, R is the gas constant and T is the temperature in K. The K_c and ΔG values are presented in Table 5. From the table it is found that the negative value of ΔG indicates the spontaneous nature of adsorption.

Other thermodynamic parameters such as entropy change (ΔS) and enthalpy change (ΔH) were determined using van't Hoff equation

Table 4
Pore diffusion coefficients for the adsorption of arsenate at various concentration and temperature

Concentration (mg/L)	Pore diffusion coefficient $D \times 10^{-9}$ (cm^2/s)
0.5	1.281
0.75	1.199
1.0	0.996
1.25	0.881
1.5	0.769
Temperature (K)	
313	1.596
323	1.429
333	1.125
343	0.899

$$\ln K_c = \frac{\Delta S}{R} - \frac{\Delta H}{RT} \quad (18)$$

The enthalpy change and entropy change were obtained from the slope and intercept of the van't Hoff linear plots of ln K_c versus 1/T, respectively (Fig. 5). A positive value of enthalpy change (ΔH) indicates that the adsorption process is endothermic in nature, and the negative value of change in internal energy (ΔG) show the spontaneous adsorption of arsenate on the adsorbent. Positive values of entropy change show the increased randomness of the solution interface during the adsorption of arsenate on the adsorbent shown in Table 6. Enhancement of adsorption capacity of electrocoagulant (magnesium hydroxide) at higher temperatures may be attributed to the enlargement of pore size and or activation of the adsorbent surface. Using Lagergren rate equation, first-order rate constants and correlation co-efficient were calculated for different temperatures (305–343 K). The calculated 'q_e' values obtained from the second-order kinetics agrees with the experimental 'q_e' values better than the first-order kinetics model. Table 6 depicts the computed results obtained from first- and second-order kinetic models. These results indicate that the adsorption follows second-order kinetic model at different temperatures used in this study.

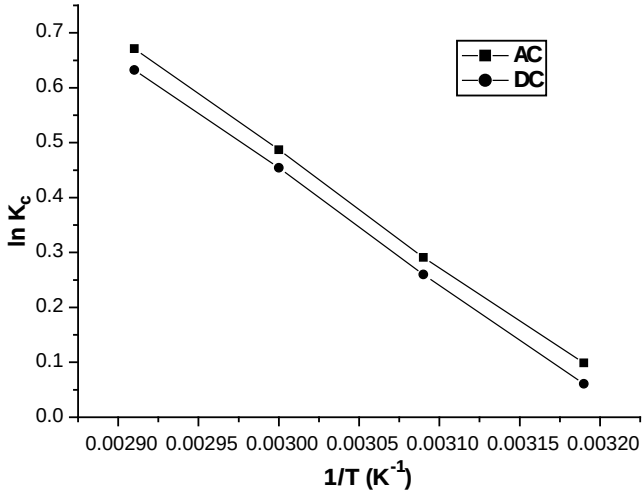

Fig. 5. Plot of ln k_c and 1/T. pH is 7.0, Current density is 0.2 A/dm^2, electrolyte temperature is 303 K and concentration is 0.5–1.5 mg/L for AC and DC.

3.7. Effect of coexisting ions

To study the effect of co-existing ions, in the removal of arsenate, sodium salts of carbonate (0–250 mg/L), phosphate (0–50 mg/L), silicate (0–15 mg/L), and fluoride (0–5.0 mg/L) were added to the electrolyte and electrolysis was carried out using AC.

3.7.1. Carbonate

Effect of carbonate on arsenate removal was evaluated by increasing the carbonate concentration from 0 to 250 mg/L in the electrolyte. The arsenate removal efficiencies are 98.3%, 98.1%, 97.6%, 67.0%, 63.4%, 46.0% and 21% for the carbonate ion concentration of 0, 2, 4, 5, 65, 150 and 250 mg/L, respectively. The results are presented in Table 7. From the removal efficiency of arsenate, it is found that the removal efficiency of the arsenate is not affected by the presence of carbonate below 5 mg/L. Significant reduction in removal efficiency was observed at and above 5 mg/L of carbonate concentration is due to the passivation of anode (hindering the dissolution process).

3.7.2. Phosphate

The concentration of phosphate ion was increased from 0 to 50 mg/L, the contaminant range of phosphate in the groundwater. The removal efficiency for arsenate was 98.3%, 89.4%, 81.7%, 62%, 47% and 32% for 0,

Table 6
Comparison between the experimental and calculated q_e values at an initial arsenate concentrations of 0.5 mg/L in first- and second-order adsorption isotherms at various temperatures

Temperature	q_e (exp)	First-order adsorption			Second-order adsorption		
		q_e (cal)	K_1 (min/mg)	R^2	q_e (cal)	K_2 (min/mg)	R^2
313	0.438	0.659	−0.0035	0.8012	0.421	0.1356	0.9999
323	0.441	0.996	−0.0025	0.8124	0.428	0.1989	0.9986
333	0.446	1.214	−0.0021	0.8324	0.435	0.2156	0.9965
343	0.451	1.326	−0.0014	0.8656	0.464	0.3197	0.9978

Table 7
Effect of addition of carbonate, phosphate, silicate and fluoride in the electrolyte for the removal of arsenate from water

Concentration (mg/L)	Removal efficiency of arsenate (%)
Carbonate	
0	98.3
2.0	98.1
4.0	97.6
5.0	67.0
65.0	63.4
150.0	46.0
250.0	21.0
Phosphate	
0	98.3
2.0	89.4
4.0	81.7
5.0	62.0
25.0	47.0
50.0	32.0
Silicate	
0	98.3
5.0	59.0
10.0	44.2
15.0	18.6
Fluoride	
0	98.3
0.2	76.0
0.5	59.0
2.0	48.0
5.0	23.5

2, 4, 5, 25 and 50 mg/L of phosphate ion respectively. The results are presented in Table 7. There is a marginal change in removal efficiency of arsenate below 5 mg L^{-1} of phosphate in the water. At higher concentrations (at and above 5 mg/L) of phosphate, the removal efficiency decreases to 45%. This is due to the preferential adsorption of phosphate over arsenate as the concentration of phosphate increase.

3.7.3. Silicate

Effect of silicate on arsenate removal was evaluated by increasing the silicate concentration from 0 to 15 mg/L in the electrolyte. The respective efficiencies for 0, 5, 10 and 15 mg/L of silicate are 98.3%, 59.0%, 44.2% and 18.6%. The removal of arsenate decreased with increasing silicate concentration from 0 to 15 mg/L. The results are presented in Table 7. In addition to preferential adsorption, it is observed that the silicate can interact with magnesium hydroxide to form soluble and highly dispersed colloids that are not removed by normal filtration.

3.7.4. Fluoride

From the results it is found that the efficiency decreased from 98.3%, 76%, 59%, 48% and 23.5% by increasing the concentration of fluoride from 0, 0.2, 0.5, 2.0 and 5.0 mg/L. The results are presented in Table 7. Like phosphate ion, this is due to the preferential adsorption of fluoride over arsenate as the concentration of fluoride increases. So, when fluoride ions are present in the water to be treated they compete greatly with arsenate ions for the binding sites.

3.8. A bench scale study

A bench scale capacity cell was designed, fabricated and operated for the removal of arsenate from water. The system consists of AC/DC power supply, an electrochemical reactor, a water tank, a feed pump, a flow control valve, a flow measuring unit, a circulation pump, settling tank, sludge collection tank, filtration unit provisions for gas outlet and treated water outlet. The reactor is made of PVC with an active volume of 2000 L. The magnesium electrodes (anode and cathode) each consists of five pieces situated approximately 5 mm apart from each other and submerged in the solution. The total electrode surface area is 1500 cm^2 for both cathode and anode. The cell was operated at a current density of 0.2 A/dm^2 and the electrolyte pH of 7.0. The results show that the removal efficiency of 98.3% and 97.9% was achieved with the energy consumption of 0.724 and 1.035 kWh/m^3 at a current density of 0.2 A/dm^2, at pH of 7.0 for AC and DC, respectively. The results were consistent with the results obtained from the laboratory scale, showing that the process was technologically feasible.

3.9. Coagulant characterization

3.9.1. SEM and EDAX studies

In order to gain more insight into the effect of alternating current, the morphology of the electrode surface after two kinds of electrolysis (AC and DC) was

characterized by SEM as shown in Fig. 6(a) and (b). It can be observed that when the AC was fed, less disordered pores formed and a smooth microstructure of magnesium suggesting the magnesium electrodes were dissolved uniformly during the electrolysis. While for the electrodes fed with DC, the electrode surface is found to be rough, with a number of dents. These dents are formed around the nucleus of the active sites where the electrode dissolution results in the production of magnesium hydroxides. The formation of a large number of dents may be attributed to the anode material consumption at active sites due to the generation of oxygen at its surface.

Energy-dispersive analysis of X-rays (EDAX) was used to analyze the elemental constituents of arsenate-adsorbed magnesium hydroxide (Fig. 7). It shows that the presence of arsenate, Mg and O appears in the spectrum. EDAX analysis provides direct evidence that arsenate is adsorbed on magnesium hydroxide.

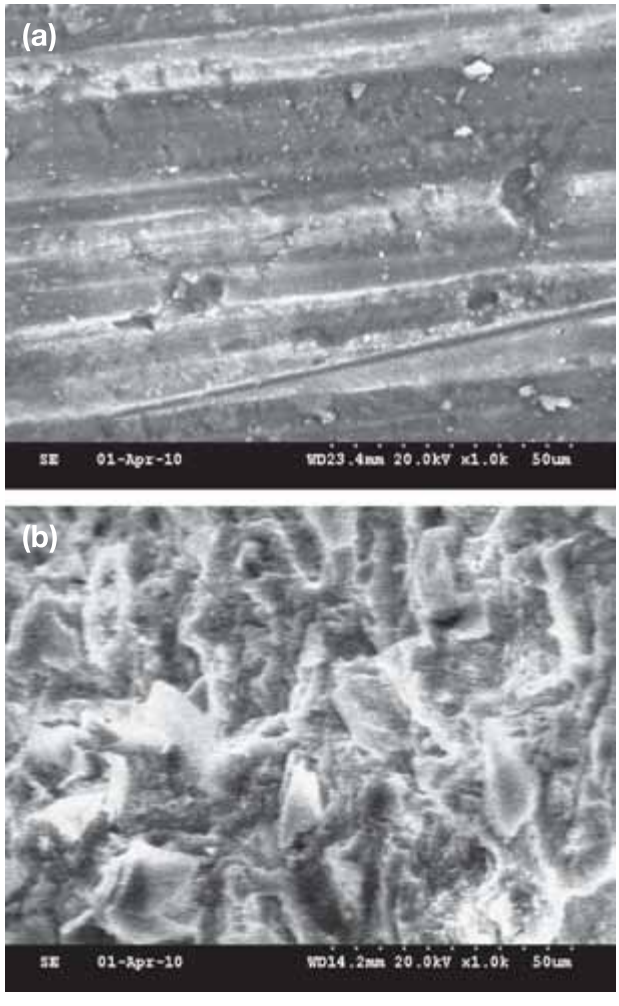

Fig. 6. SEM images of the anode after electrocoagulation by (a) AC and (b) DC.

3.9.2. FTIR and XRD studies

Fig. 8 presents the FTIR spectrum of arsenate–magnesium hydroxide. A broad adsorption band at 3452.84 cm^{-1} implies the transformation from free protons into

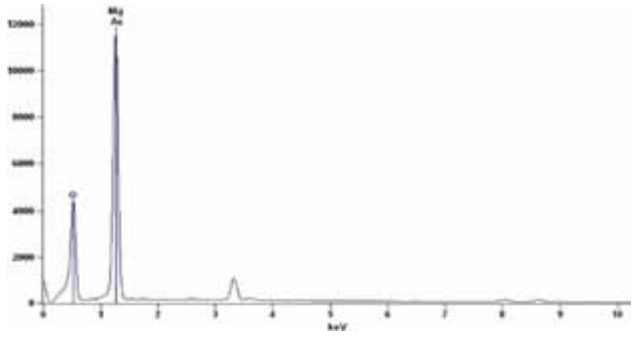

Fig. 7. EDAX spectrum of arsenate-adsorbed magnesium hydroxide.

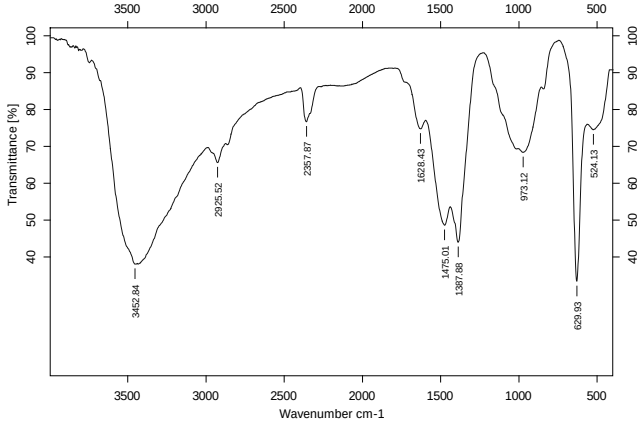

Fig. 8. FT-IR spectrum for arsenate-adsorbed magnesium hydroxide.

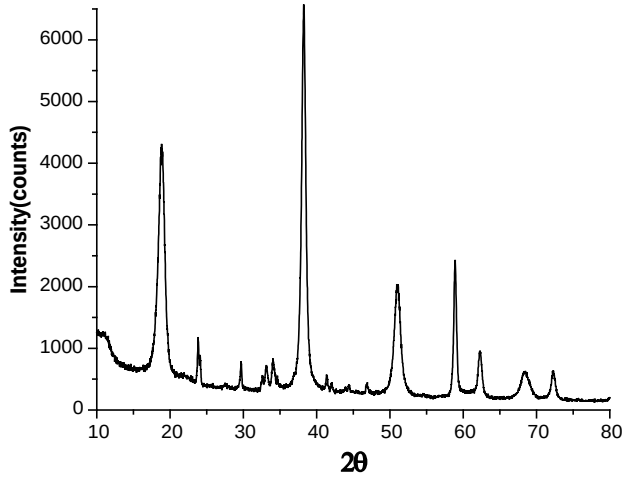

Fig. 9. XRD spectrum for arsenate-adsorbed magnesium hydroxide.

a proton-conductive state in brucite. The 1628.43 cm^{-1} peak indicates the bent vibration of H–O–H. The band at 629.93 cm^{-1} corresponds to Mg–O stretching vibration. Electrocoagulation by-product showed the well crystalline phase of magnesium hydroxide (Fig. 9).

4. Conclusions

The results showed that the optimized removal efficiency of 98.3% and 97.9% was achieved for AC and DC source at a current density of 0.2 A/dm^2 and pH of 7.0 using magnesium electrodes. The magnesium hydroxide generated in the cell remove the arsenate present in the water and to reduce the arsenate concentration to less than 0.005 mg/L, and made it for drinking. The bench scale results showed that the process was technologically feasible. For both AC and DC electrolysis the adsorption of arsenate preferably fitting Langmuir adsorption isotherm. The adsorption process follows second-order kinetics. Temperature studies showed that adsorption was endothermic and spontaneous in nature. From the surface characterization studies, it is confirmed that the magnesium hydroxide generated in the cell adsorbed arsenate present in the water.

Acknowledgment

The authors wish to express their gratitude to the Director, Central Electrochemical Research Institute, Karaikudi to publish this paper.

References

[1] F.S. Zhang and H. Itoh. Chemosphere, 60 (3) (2005) 319–325.
[2] D. Mohan and C.U. Pittman Jr. J. Hazard. Mater., 142 (1–2) (2007) 1–53.
[3] H.S. Altundogan, S. Altundogan, F. Tumen and M. Bildik. Waste Manage., 22 (3) (2002) 357–363.
[4] A. Manning, E. Fendorf and S. Goldberg. Environ. Sci. Technol., 32 (16) (1998) 2383–2388.
[5] T. Stanic, A. Dakavic, A. Zivanovic, M. Canovic, Vera Dondur and S. Milicevic. Environ. Chem. Lett., 7 (2008) 161–166.
[6] USEPA, National primary drinking water regulations; arsenic and clarification to contaminants monitoring, vol. 66,2001, pp. 6975–7066.
[7] B. Dousava, V. Machovic, D. Kolousek, F. Kovanda and V. Dornicak. Water, Air, Soil Pollut., 49 (2003) 251–269.
[8] C. Namashivayam and S. Senthilkumar. Ind. Eng. Chem. Res., 37 (12) (1998) 4816–4822.
[9] N. Seko, F. Basuki, M. Tamada and F. Yoshii. React. Funct. Polym., 59 (3) (2004) 235–241.
[10] L. Zeng. Water Res., 37 (18) (2004) 4351–4358.
[11] M.T. Emett and G.H. Khoe. Water Res., 35 (3) (2001) 649–656.
[12] S.M. Fendorf, J. Eick, P.R. Grossl and D.L. Sparks. Environ. Sci. Tech., 31 (2) (1997) 315–320.
[13] Y. Zhang, M. Yang and X. Huang. Chemosphere, 51 (9) (2003) 945–952.
[14] Y.H. Xu, T. Nakajima and A. Ohki. J. Hazard. Mater., B92 (3) (2002) 275–287.
[15] P. Ratna kumar, C. Sanjeev, C. Khilar and S.P. Mahajan. Chemosphere, 55 (9) (2004) 1245–1252.
[16] X. Xu and X. Zhu. Chemosphere, 56 (10) (2004) 889–894.
[17] X. Chen, G. Chen and P.L. Yue. Chem. Eng. Sci., 57 (13) (2002) 2449–2455.
[18] G. Chen. Sep. Purif. Technol., 38 (1) (2004) 11–41.
[19] N. Adhoum and L. Monser. Chem. Eng. Process, 43 (10) (2004) 1281–1287.
[20] K. Rajeshwar and J.K. Ibanez. Environmental Electrochemistry: Fundamentals and Applications in Pollution Abatement, Academic Press: San Diego, 1997.
[21] E.A. Vik, D.A. Carlson, A.S. Eikum and E.T. Gjessing. Water Res., 18 (11) (1984) 1355–1360.
[22] E. Onder, A.S. Koparal and U.B. Ogutveren. Sep. Purif. Technol., 52 (3) (2007) 527–532.
[23] M. Ikematsu, K. Kaneda, M. Iseki and M. Yasuda. Sci. Total Environ., 382 (1) (2007) 159–164.
[24] P.A. Christensen, T.A. Egerton, W.F. Lin, P. Meynet, Z.G. Shaoa and N.G. Wright. Chem. Commun., 38 (2006) 4022–4023.
[25] A. Carlos, M. Huitle and S. Ferro. Chem. Soc. Rev., 35 (2006) 1324–1340.
[26] S. Vasudevan, J. Lakshmi and G. Sozhan. Clean, 37 (1) (2009) 45–51.
[27] B.R. Manna, S. Debnath, J. Hossain and U.C. Ghosh. Indus. Pollut. Cont., 20 (2) (2004) 247–266.
[28] B. Manna and U.C. Ghosh. J. Hazard. Mater.,144 (1–2) (2007) 522–531.
[29] K.P. Raven, A. Jain and R.H. Loeppert. Environ. Sci. Tech., 32 (1998) 344–349.
[30] D. Erhan, M. Kobya, S. Elif and T. Ozkan. Water SA., 30 (2004) 533–540.
[31] I.A. Oke, N.O. Olarinoye and S.R.A. Adewusi. Adsorption, 14 (1) (2008) 85–92.
[32] W.J. Weber Jr. and J.C. Morris. J. Sanit. Div. Am. Soc. Civ. Eng., 89 (SA2) (1963) 31–59.
[33] S.J. Allen, G. Mckay and K.H.Y. Khader, Environ. Pollut,. 56 (1) (1989) 39–50.
[34] M.S. Gasser, G.H.A. Morad, H.F. Aly. J. Hazard. Mater., 142 (1–2) (2007) 118–129.
[35] M. Jaroniec. Adv. Colloid Interface Sci., 18 (1983) 149–225.
[36] B.R. Manna, M. Dasgupta and U.C. Ghosh. Water SRT-AQUA., 53 (7) (2004) 483–495.
[37] Y.S. Ho and G. McKay. Water Res., 33 (2) (1999) 578–584.
[38] I.A.W. Tan, B.H. Hameed and A.L. Ahmed. Chem. Eng. J., 127 (1–3) (2007) 111–119.
[39] H. Demiral, I. Demiral, F. Tumsek and B. Karacbacakoglu. Chem. Eng. J., 144 (3) (2008) 184–188.
[40] E. Oguz. Colloid Surf., A 252 (2–3) (2005) 121–128.
[41] N.K. Lazaridis, D.N. Bakayannakis and E.A. Deliayanni. Chemosphere, 58 (11) (2005) 65–73.
[42] X.Y. Yang and B. Al-Duri. Chem. Eng. J., 83 (1) (2001) 15–23.
[43] A.K. Golder, A.N. Samantha and S. Ray. Sep. Purif. Technol., 52 (1) (2006) 102–109.